Supplementary Material

Supplementary figure legends

Fig. S1: Characterisation of human brain organoids and expression of FOXG1

(A) Immunostainings of control organoid slices after 105 days in culture presenting different markers (Paired box protein (PAX6), Neuron-specific class III beta-tubulin (TUJ), neuronal nuclei (NeuN), glial fibrillary acidic protein (GFAP), vesicular glutamate transporter 1 (vGLUT1), vGLUT2, T-box brain transcription factor 1 (TBR1), TBR2) of neural development. Scale bars as indicated in the figures.

(B) Immunostainings of FOXG1 in CO of healthy donor (HD) and FOXG1del showing reduced FOXG1 protein expression in FOXG1del compared to HD after 105 d ays in culture. Dashed line delineates the organoid surface. Scale bars as indicated in the figure.

Fig. S2: FOXG1 associates with RNA

(A) Upper part: Different transcript variants of *Map1b* (orange). Boxes represent the different exons.

Lower part: RIPseq tracks of $\log_2$(foldchange) (LFC) of reads in FOXG1-coIP vs IgG-coIP in the different n (green) and the average of those LFCs (black) in the genomic region of *Map1b.* On the x-axis the position on the corresponding chromosome is indicated in bp of the mm10 genome.

(B) Upper part: Different transcript variants of *Pantr1* (orange). Boxes represent the different exons.

Lower part: RIPseq tracks of $\log_2$(foldchange) (LFC) of reads in FOXG1-coIP vs IgG-coIP in the different n (green) and the average of those LFCs (black) in the genomic region of *Pantr1.* On the x-axis the position on the corresponding chromosome is indicated in bp of the mm10 genome.

Fig. S3: FOXG1 localises in the vicinity of *PANTR1* in vivo

(A) Overview of the expression of *PANTR1* (smFISH) and FOXG1 protein in human d105 brain organoids. The boxed area indicates the magnification shown in Fig. 4F.

(B) Mouse brain (P0) stained with smFISH probe targeting *Pantr1* (green) and immunostained for FOXG1 (red). Boxed area indicates the magnification shown in Fig.

4G. Scale bars as indicated in the figure.

Fig. S4: Analyses of FOXG1-ChIPseq peaks upon *Pantr1*KD in DIV7 primary mouse hippocampal neurons

(A) Heatmap of regions 5 Kb up-/downstream of all identified FOXG1 peak summits, represented as k-means clusters with k=4 in control (Ctrl) and *Pantr1*KD condition as well as the comparison of both conditions. Data are normalised by sequencing depth and input control as $\log_2$(ChIP/Input) for Ctrl and *Pantr1*KD data. The difference between *Pantr1*KD and control condition was calculated from RPKM normalised bigwig files as $\log_2$ (Pantr1KD/Control). The metaprofiles (top) show the mean $\log_2$FC (LFC) of each cluster. n=2.

(B) GO-term enrichment of the genes in proximity to the FOXG1 ChIPseq summits broken down to the different clusters upon *Pantr1*KD in DIV7 primary hippocampal neurons as shown in (A) with a q-value cutoff of 0.05 and p-value cutoff of 0.05.

(C) Heatmap of common DEGs in the RNAseq data sets after *Foxg1*KD (adjusted p-value (padj) < 0.05 and an LFC < -0.584 or > 0.584) and annotated genes (ChIPSeeker) corresponding to all DBRs in the FOXG1-ChIPseq data set upon *Pantr1*KD. Shown are the LFC compared to the control condition. Genes connected to neurite outgrowth and neural development are marked with a yellow box.

(D) Motifs analysis of the summits in the different clusters as shown in (A). Shown is a heatmap of the aggregated z-scores.

Fig. S5: FOXG1 binding profiles at *Pantr1*-dependent FOXG1 target genes in mouse hippocampal cells

Shown are bigwig tracks of FOXG1 binding sites upon FOXG1 ChIPseq as LFC towards input samples from murine adult hippocampus *in vivo*, and *in vitro* E18.5 cultured primary hippocampal neurons at DIV11 (hipp. primary neurons) [1], E18.5 cultured primary hippocampal neurons at DIV7 (DIV7 control) and upon *Pantr1* KD (DIV7 *Pantr1*KD) as well as the ratio of coverage upon *Pantr1*KD vs control condition (*Pantr1*KD/control). Selected genes classify as *Pantr1*-dependent FOXG1 target genes. The last track displays the binding region called as significant DBR upon *Pantr1* KD. Peak sequences of the DBRs and surrounding loci are marked with a red box. On the x-axis the position on the corresponding chromosome is indicated in bp of the mm10 genome.

Fig. S6: FOXG1 binding to *Pantr1*-dependent target genes in human cortical organoids

(A) ChIPseq of FOXG1 in human cortical organoids (d105, hCO) showing distribution of enriched FOXG1 peaks of the 13 mouse *Pantr1*-dependent FOXG1 target genes. Red boxes indicate the localisation of the respective DBR of FOXG1 upon *Pantr1*KD in mouse cells as shown in Fig. S6. The last track indicate predicted FOXG1 binding motifs at the respective chromosomal location. On the x-axis the position on the corresponding chromosome is indicated in bp of the hg38 genome. Mapped tracks show the $\log_2$(foldchange) (LFC) over the input sample for each condition.

(B) Violin plots of cell-type specific expression levels of *SLC8A1*. *SLC8A1* expression reduced significantly upon *FOXG1* deletion in ventricular and outer radial glia highlighted in brownish colour, and in the migrating IN II as highlighted in violet.

figure S1

A

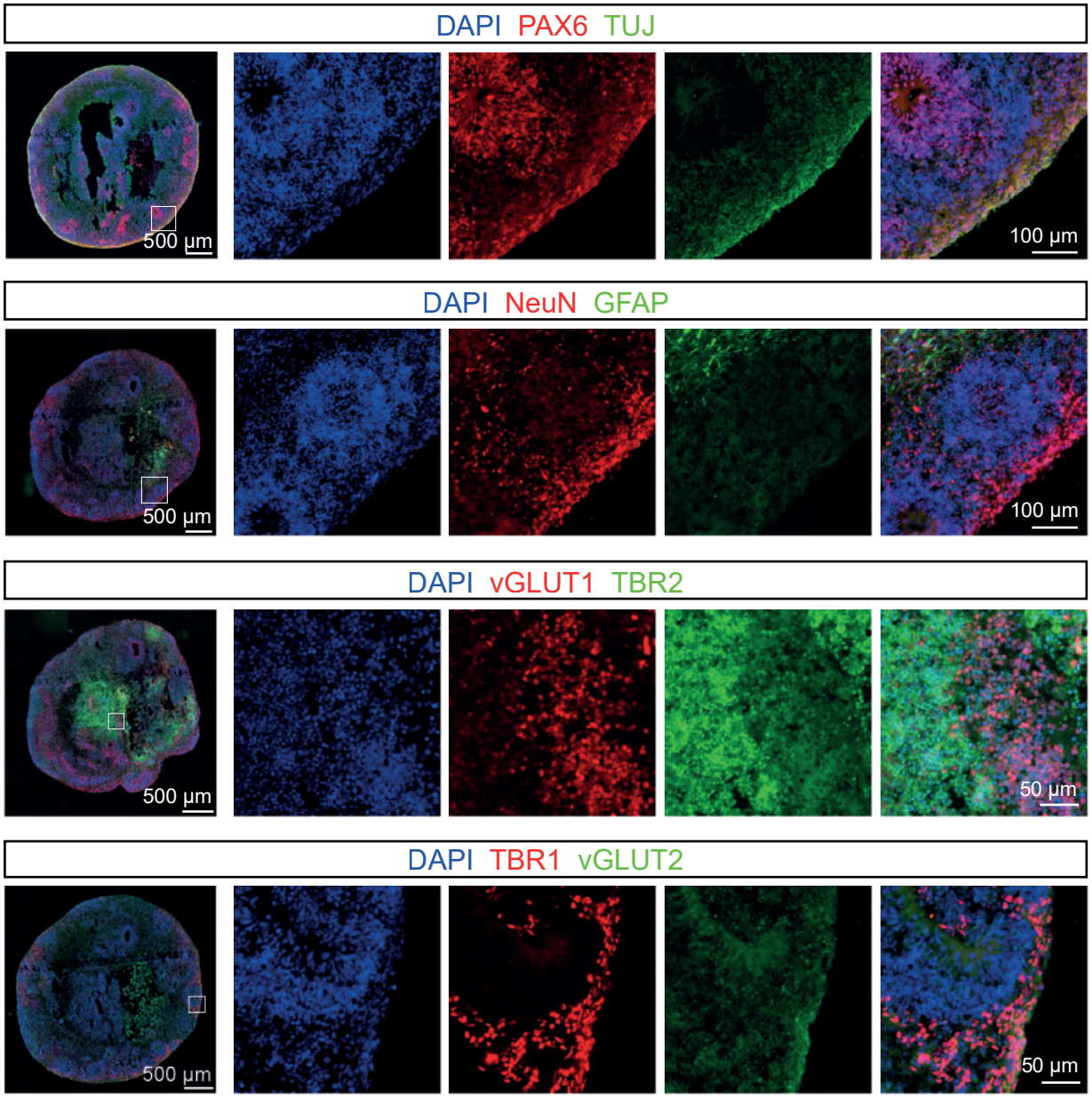
DAPI PAX6 TUJ
500 µm
100 µm
DAPI NeuN GFAP
500 µm
100 µm
DAPI vGLUT1 TBR2
500 µm
50 µm
DAPI TBR1 vGLUT2
500 µm
50 µm

B

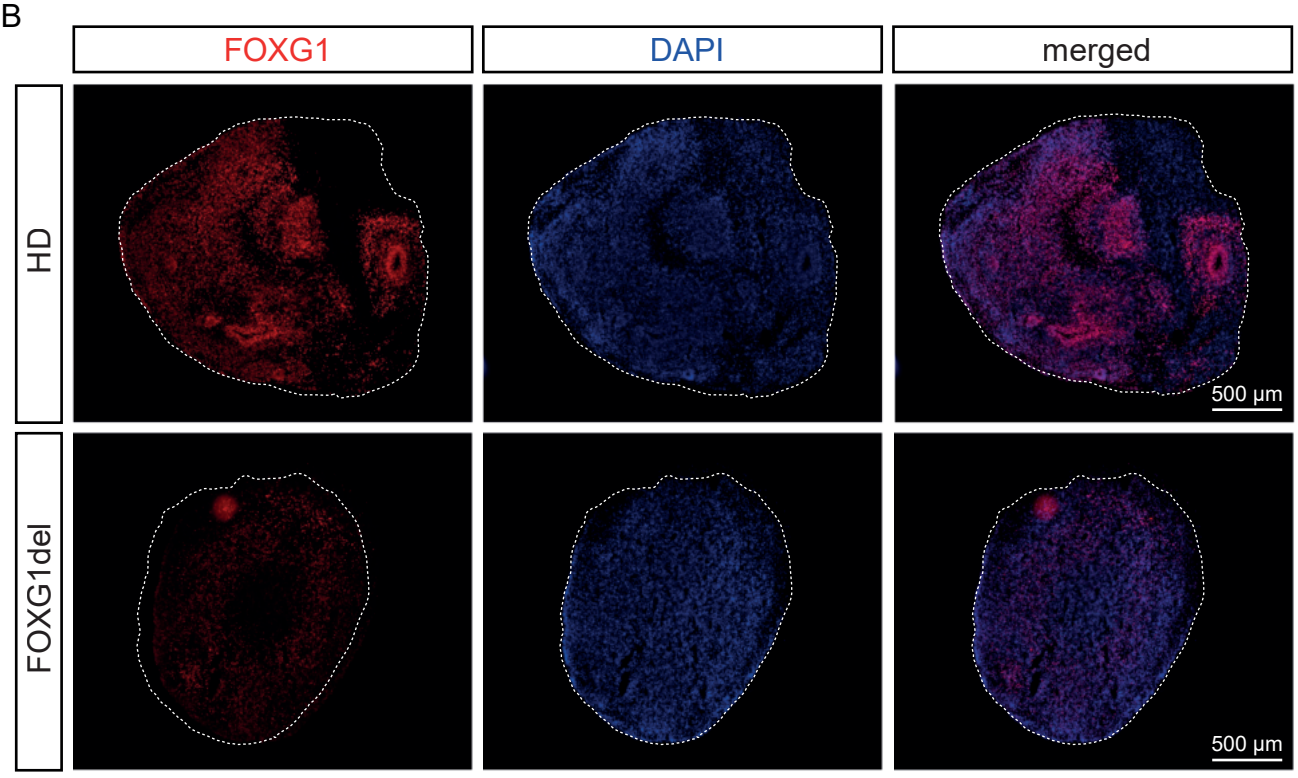
FOXG1
DAPI
merged
HD
FOXG1del
500 µm
500 µm

figure S2

A

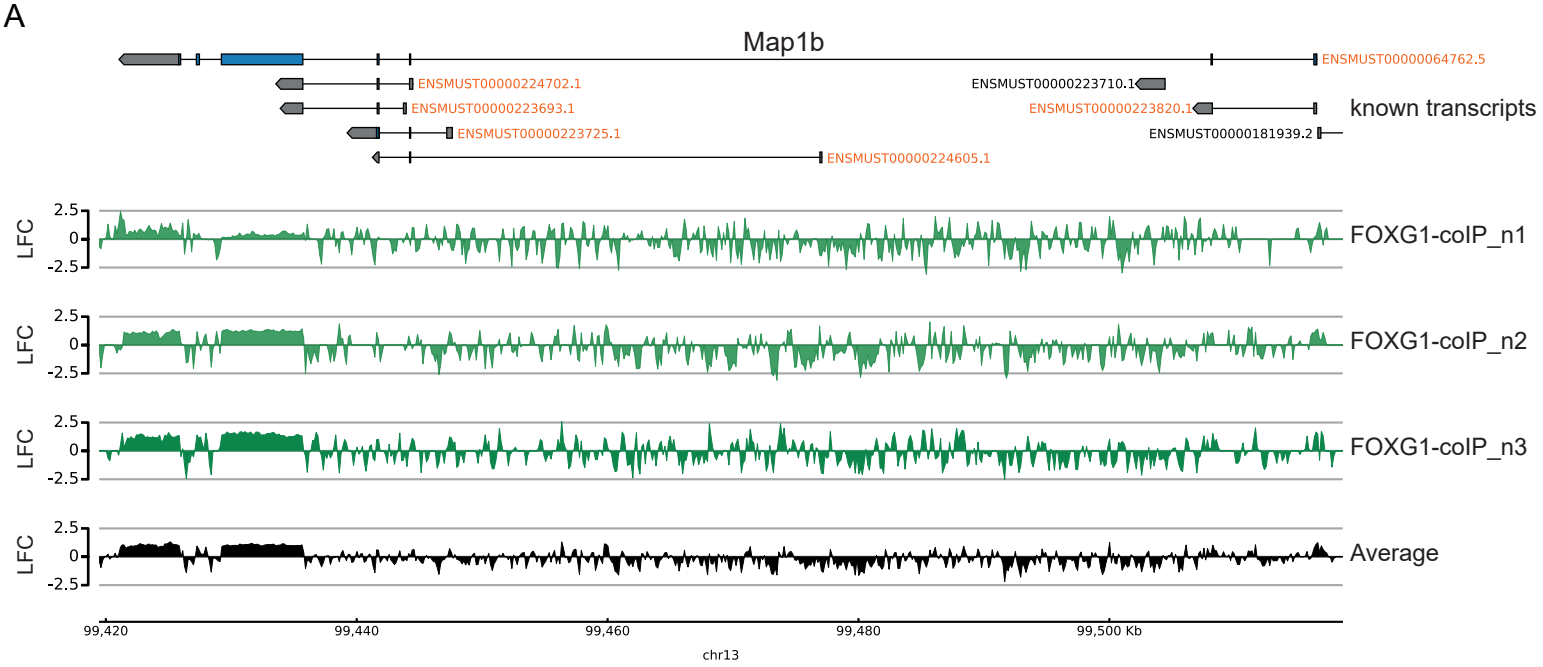
Map1b
ENSMUST00000064762.5
ENSMUST00000224702.1
ENSMUST00000223710.1
ENSMUST00000223693.1
ENSMUST00000223820.1
known transcripts
ENSMUST00000223725.1
ENSMUST00000181939.2
ENSMUST00000224605.1
LFC
2.5
0
-2.5
FOXG1-coIP_n1
FOXG1-coIP_n2
FOXG1-coIP_n3
Average
99,420
99,440
99,460
99,480
99,500 Kb
chr13

B

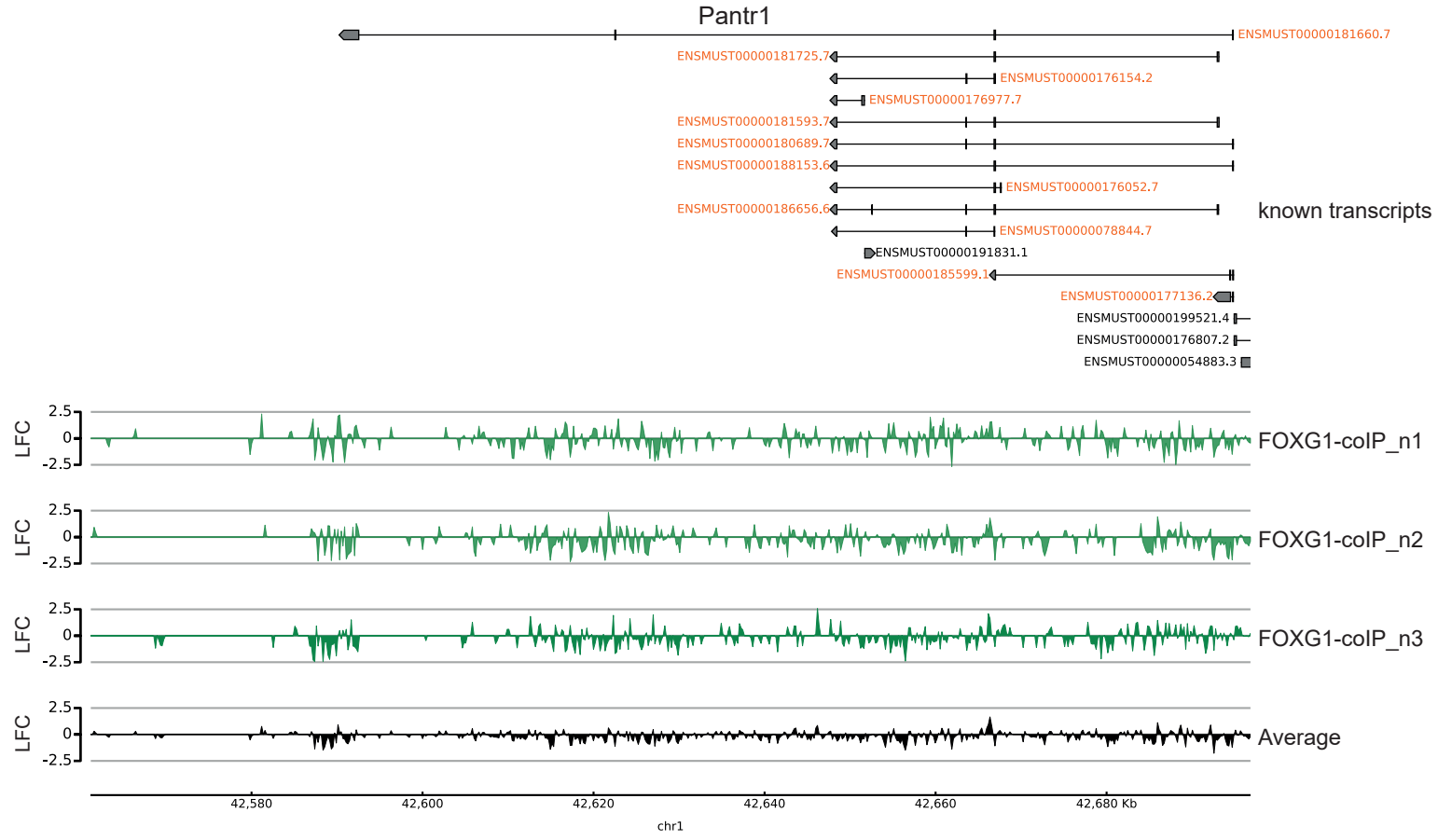
Pantr1
ENSMUST00000181660.7
ENSMUST00000181725.7
ENSMUST00000176154.2
ENSMUST00000176977.7
ENSMUST00000181593.7
ENSMUST00000180689.7
ENSMUST00000188153.6
ENSMUST00000176052.7
ENSMUST00000186656.6
known transcripts
ENSMUST00000078844.7
ENSMUST00000191831.1
ENSMUST00000185599.1
ENSMUST00000177136.2
ENSMUST00000199521.4
ENSMUST00000176807.2
ENSMUST00000054883.3
LFC
2.5
0
-2.5
FOXG1-coIP_n1
FOXG1-coIP_n2
FOXG1-coIP_n3
Average
42,580
42,600
42,620
42,640
42,660
42,680 Kb
chr1

figure S3

A

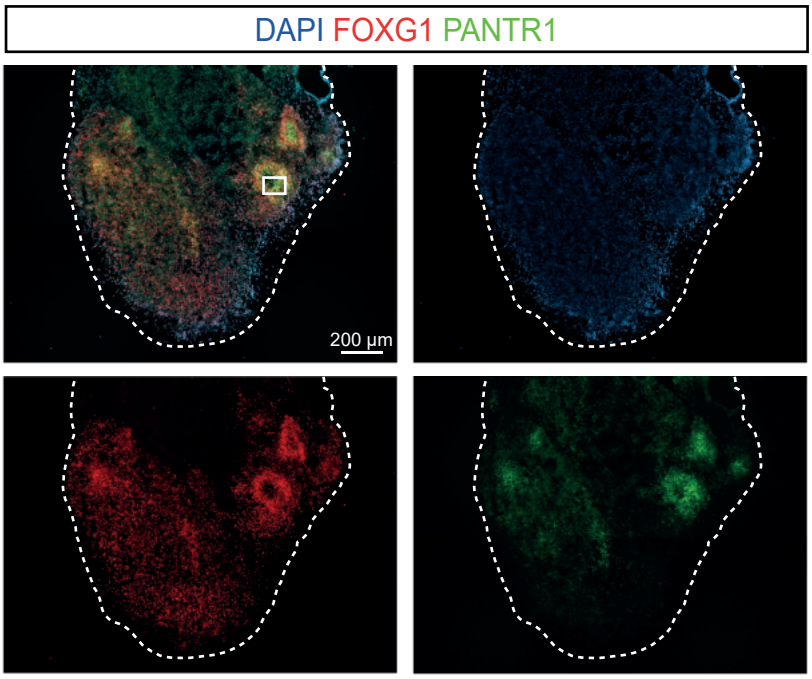

B

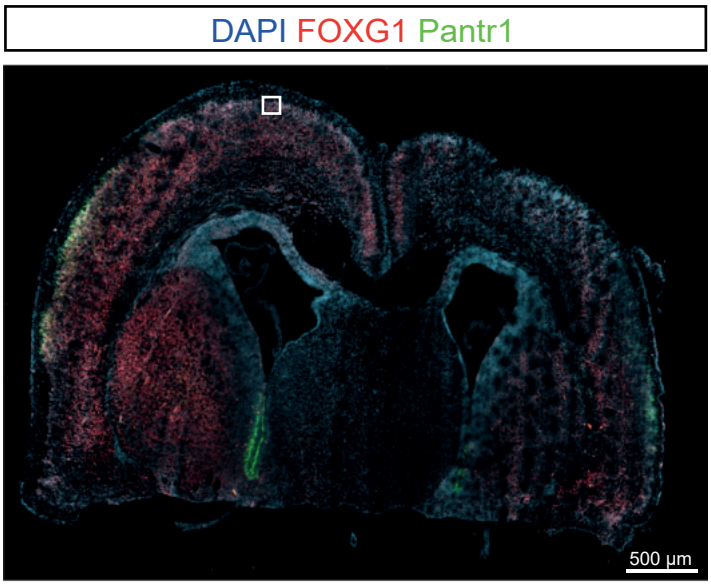

figure S4

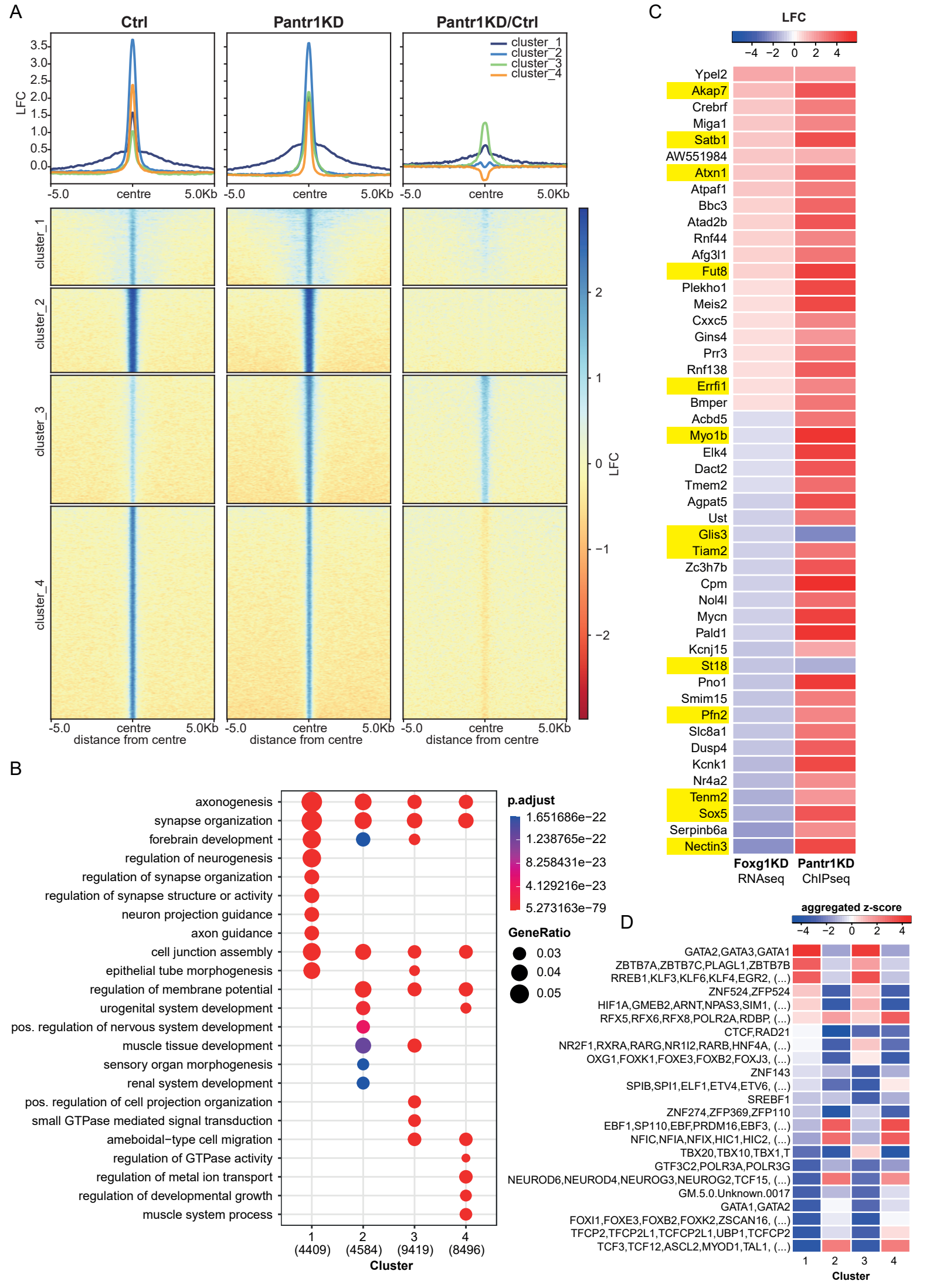
A
Ctrl
Pantr1KD
Pantr1KD/Ctrl
cluster_1
cluster_2
cluster_3
cluster_4
LFC
-5.0
centre
5.0Kb
distance from centre
B
axonogenesis
synapse organization
forebrain development
regulation of neurogenesis
regulation of synapse organization
regulation of synapse structure or activity
neuron projection guidance
axon guidance
cell junction assembly
epithelial tube morphogenesis
regulation of membrane potential
urogenital system development
pos. regulation of nervous system development
muscle tissue development
sensory organ morphogenesis
renal system development
pos. regulation of cell projection organization
small GTPase mediated signal transduction
ameboidal−type cell migration
regulation of GTPase activity
regulation of metal ion transport
regulation of developmental growth
muscle system process
p.adjust
1.651686e−22
1.238765e−22
8.258431e−23
4.129216e−23
5.273163e−79
GeneRatio
0.03
0.04
0.05
1 (4409)
2 (4584)
3 (9419)
4 (8496)
Cluster
C
LFC
Ypel2
Akap7
Crebrf
Miga1
Satb1
AW551984
Atxn1
Atpaf1
Bbc3
Atad2b
Rnf44
Afg3l1
Fut8
Plekho1
Meis2
Cxxc5
Gins4
Prr3
Rnf138
Errfi1
Bmper
Acbd5
Myo1b
Elk4
Dact2
Tmem2
Agpat5
Ust
Glis3
Tiam2
Zc3h7b
Cpm
Nol4l
Mycn
Pald1
Kcnj15
St18
Pno1
Smim15
Pfn2
Slc8a1
Dusp4
Kcnk1
Nr4a2
Tenm2
Sox5
Serpinb6a
Nectin3
Foxg1KD RNAseq
Pantr1KD ChIPseq
D
aggregated z-score
GATA2,GATA3,GATA1
ZBTB7A,ZBTB7C,PLAGL1,ZBTB7B
RREB1,KLF3,KLF6,KLF4,EGR2, (...)
ZNF524,ZFP524
HIF1A,GMEB2,ARNT,NPAS3,SIM1, (...)
RFX5,RFX6,RFX8,POLR2A,RDBP, (...)
CTCF,RAD21
NR2F1,RXRA,RARG,NR1I2,RARB,HNF4A, (...)
OXG1,FOXK1,FOXE3,FOXB2,FOXJ3, (...)
ZNF143
SPIB,SPI1,ELF1,ETV4,ETV6, (...)
SREBF1
ZNF274,ZFP369,ZFP110
EBF1,SP110,EBF,PRDM16,EBF3, (...)
NFIC,NFIA,NFIX,HIC1,HIC2, (...)
TBX20,TBX10,TBX1,T
GTF3C2,POLR3A,POLR3G
NEUROD6,NEUROD4,NEUROG3,NEUROG2,TCF15, (...)
GM.5.0.Unknown.0017
GATA1,GATA2
FOXI1,FOXE3,FOXB2,FOXK2,ZSCAN16, (...)
TFCP2,TFCP2L1,TCFCP2L1,UBP1,TCFCP2
TCF3,TCF12,ASCL2,MYOD1,TAL1, (...)
Cluster

figure S5


Nr4a2
Ust
Crebrf
Cpm
Miga1
St18
Satb1
Slc8a1
Atxn1
Dusp4
Atad2b
Afg3l1p
Rfn44
Refseq
RPKM
adult hippocampus
hipp. primary neurons
LFC
DIV7 control
DIV7 Pantr1KD
Pantr1KD/control
DBR after Pantr1KD

figure S6

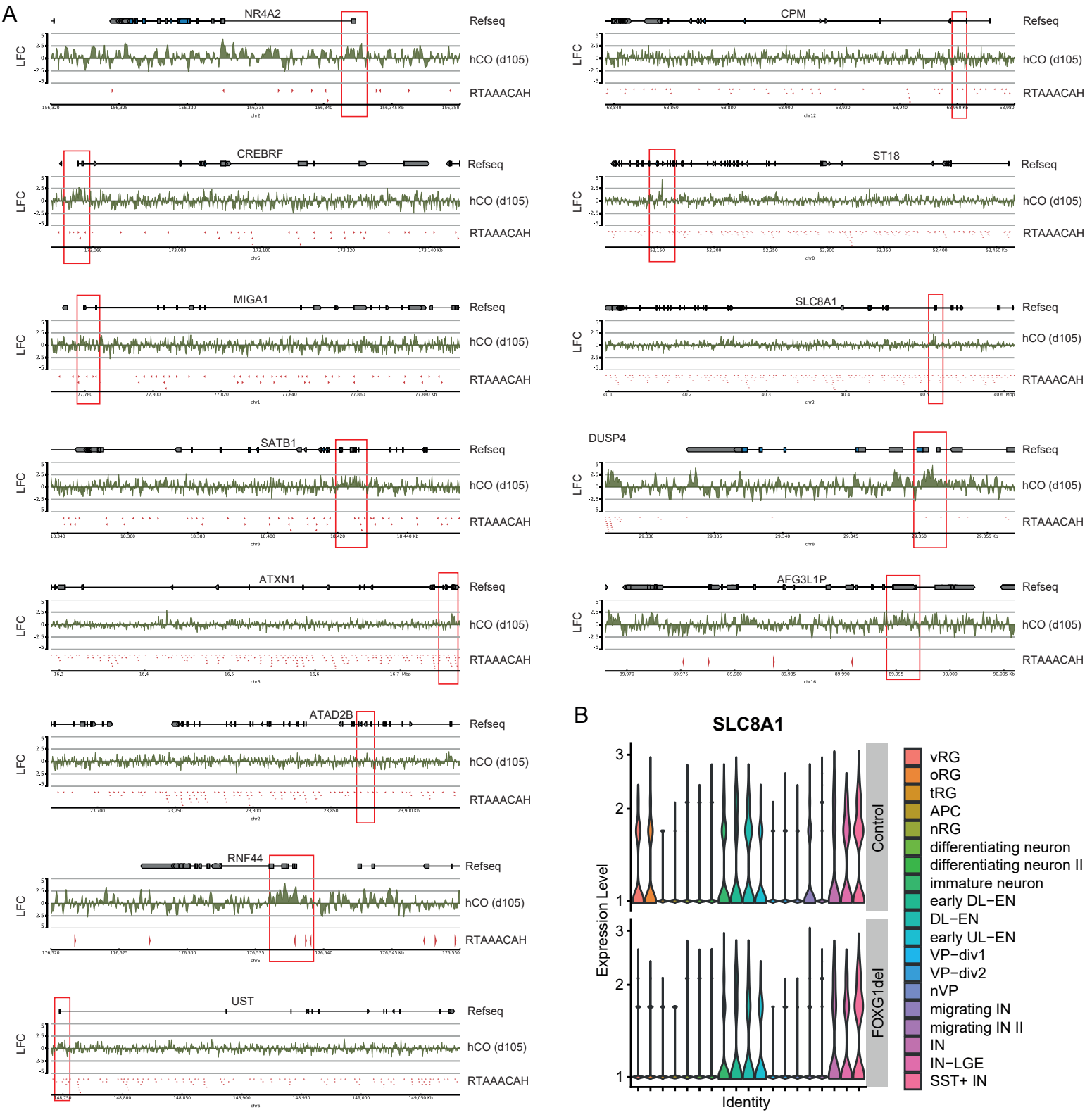
A
NR4A2
CPM
CREBRF
ST18
MIGA1
SLC8A1
SATB1
DUSP4
ATXN1
AFG3L1P
ATAD2B
RNF44
UST
Refseq
hCO (d105)
RTAAACAH
LFC
B
SLC8A1
Expression Level
Identity
Control
FOXG1del
vRG
oRG
tRG
APC
nRG
differentiating neuron
differentiating neuron II
immature neuron
early DL−EN
DL−EN
early UL−EN
VP−div1
VP−div2
nVP
migrating IN
migrating IN II
IN
IN−LGE
SST+ IN

Supplementary Material and Methods

Mouse tissue isolation for RNAseq

Cortex of E13.5 embryos were dissected from Foxg1$^{cre/cre}$ and wildtype mice (Foxg1$^{+/+}$), hippocampi of E18.5 embryos and adult mice were isolated from Foxg1$^{cre/+}$ and wildtype mice (Foxg1$^{+/+}$). Tissue was subsequently used for RNAseq. Foxg1 lines have C57BL/6J background and are described by the producers [2], (https://www.jax.org/strain/004337).

Mouse hippocampus isolation for primary neuronal culture

Hippocampi of E18.5 embryos and P0 mice were dissected from wildtype mice (C57BL/6J or CD1 with animal license X-17/03S and X-22/02B, Charles River) and collected in 15 ml Hanks' Balanced Salt Solution (HBSS, PAA, Germany). The tissue was processed for plating as previously described [3,4]. Cells were plated at a density of 100.000 cells/cm^2 for RNA extraction or 50.000 cells/cm^2 for microscopy and electrophysiological recordings. Medium change was performed every 72 h by exchanging half of the volume of the medium with fresh NB medium with complements and AraC (1 µg/ml for the first, and 0.5 µg/ml for the second medium change, Sigma/Merck, Germany), cells were harvested at DIV7 (ChIPseq, RIP, RNAseq) (RNAseq) and DIV14 (electrophysiology) based on the performed experiments.

Production of lentiviral particles and transduction

Lentiviral particles were produced and quantified in HEK293T cells with Mirus TransIT-293 Transfection Reagent (Mirus Bio LLC, Madison, WI, USA) as described before [3]. The constructs used are listed in Supplemental Table S1. Constructs for lentiviral packaging were pMD2.G (Didier Trono, plasmid #12259, Addgene, USA) and psPAX2 (Didier Trono, plasmid #12260, Addgene, USA). Primary hippocampal cells were virally transduced at DIV1 with 1.25 IFU/cell (shRNA-mediated KD as well as rescue with Pantr1 overexpression). Selection of successfully infected cells was performed 72-90 h post-infection (DIV4) by changing half of the volume of the medium with fresh NB medium containing 0.3 µg/ml Puromycin (Sigma/Merck, Germany).

RNA isolation, reverse transcription, and quantitative real-time PCR analysis

RNA was isolated from tissue, organoids, cell samples or coIP beads with the RNAeasy Mini Kit (#74104, Qiagen, Germany) including an on-column DNAse digestion (#79254, Qiagen, Germany). The isolated RNA was either used for further RNAseq or for quantitative real-time PCR (qRT-PCR) analysis. For qRT-PCR analysis, we harvested 1 Mio cells or one organoid in RTL buffer (#74104, Qiagen, Germany). cDNA was synthesized with the RevertAid Reverse Transcriptase kit (EP0442, Thermo

Scientific, Lithuania) and subsequently used for a qRT-PCR with GoTaq® qPCR Master Mix (A6002, Promega, WI, USA) following the manufacturer's protocol. Primers (Sigma/Merck, Germany) are listed in Supplemental Table S2. qRT-PCR after coIP was performed with three technical replicates and the ct values were used to calculate the percentage of RNA left after co-IP compared to the cell lysate (input). All other analyses were performed as described before [3]. Data are presented as mean ± SEM. P-values were calculated using unpaired, two tailed Student's t-test or one-way ANOVA: *p < 0.05, **p < 0.01, ***p < 0.001 with GraphPad Prism 6.

Immunoblotting (IB)

Co-immunoprecipitation (Co-IP) samples were loaded onto 10% SDS-polyacrylamide gels and electrophoresed at 120 V for 1.5 h in Tris-Glycine running buffer. Subsequently, proteins were transferred onto PVDF membranes (Trans-blot Turbo Transfer Pack, Bio-Rad, USA) using the Trans-blot Turbo Transfer System (Bio-Rad, USA), following the manufacturer's instructions. Afterwards, the membranes were blocked with 5% BSA (Roth, Germany) in Tris-buffered saline (TBS) for 1 h. For immunoblotting, the following antibodies were utilized: anti-FOXG1 (anti-FOXG1, #61211, Active Motif, Carlsbad, CA, USA), diluted in 5% BSA in TBST (Tris-buffered saline with 0.1% Tween-20 (Merck, Germany)). After three washes with TBST, the membranes were incubated with Tidyblot (diluted 1:5000 in 5% BSA in TBST, Biorad, USA), for 1 h. Following two washes with TBST and two with TBS, the membranes were developed using SuperSignal™ West Femto Maximum Sensitivity Substrate (Thermo Scientific, USA) and imaged with the LAS ImageQuant System (GE Healthcare, USA).

Immunohistochemistry (IHC)

Isolated mouse brains (E18.5 or P0) were fixed for 24 h, human cerebral organoids were fixed for 60 min in 4% PFA. Afterwards the tissues were incubated in 30% sucrose in DPBS (14190-094, Gibco, United Kingdom) overnight at 4°C and were subsequently embedded in tissue freezing medium (Leica, Richmond, USA). Frozen embedded tissues were cut in 14 µm sections and mounted on SuperFrost Plus Microscope slides (Thermo Scientific, Germany). Dried slides were washed two times with DPBS (14190-094, Gibco, United Kingdom), incubated 30 min with 0.25% Triton X (Roth, Germany) in DPBS and 5 min with 0.25% Triton X in DPBS. Blocking was performed in 10% normal donkey serum (017-000-121, Jackson Immuno Research, United Kingdom), 0,1% Triton X in DPBS for 2 h at RT, followed by the incubation with primary antibodies in blocking solution at 4°C overnight. After three washing steps in 0,1% Triton X in DPBS, the cover slips were incubated with secondary antibodies for 1 h at RT (dilution 1:500 in blocking solution), followed by counterstaining with DAPI (1:1000, D9542, Sigma Aldrich, Germany), three additional washing steps with DPBS and mounting in Fluorescent Mounting Medium (DAKO, S3023, Agilent, US). The

antibodies used are listed in Supplemental Table S3.

Immunocytochemistry (ICC)

For ICC, 50.000 cells plated on coverslips were fixed for 15 min with 4% PFA (MC1040051000, Merck, Germany). Blocking was performed in 10% normal goat serum (G6767, Sigma Aldrich, Germany) and 0,1% Triton X (Roth, Germany) in DPBS (14190-094, Gibco, United Kingdom) for 15 min at RT, followed by the incubation with primary antibodies in blocking solution at 4°C overnight. After three washing steps in DPBS, the cover slips were incubated with secondary antibodies for 1 h at RT, followed by counterstaining with DAPI (1:1000, D9542, Sigma Aldrich, Germany) and mounting in Fluorescent Mounting Medium (DAKO, S3023, Agilent, US). The antibodies used are listed in Supplemental Table S3.

Microscopy and morphometric analysis

DIV7 hippocampal neurons stained with MAP2 (1:200, ab32454, abcam, United Kingdom) were imaged with the microscope Axio Imager M2, objective EC Plan NeoFluar 40x/0.75 M27, Axiocam 506, software ZEN 3.0. Dendrites were traced manually using the Sholl-analysis plugin for ImageJ 1.52p by a second experimenter blindly. Dendrite complexity was assessed by measuring the dendritic intersections in concentric circles per 10 µm from the cell soma and significance was determined using two-way ANOVA test.
For dendritic spine density analysis, biocytin-filled neurons were stained with Alexa Fluor™ 633-conjugat (1:500, S21375, Life Technologies, USA), Z-stack pictures were acquired using SP8 confocal microscope, objective HC PL APO CS2 63x/1.40 OIL, zoom 2x and resolution 2048 x 2048. The analysis was performed by counting spines on 20 µm length dendrite, 3 dendrites for each neuron were quantified using LAS X 3.5.2.18963**.**
For localization and co-localization studies Z-stack pictures were acquired using SP8 confocal microscope, objective Zeiss HC PL APO CS2 63x/1.40 OIL, pixel size 0.361 x 0.361 µm and analysis was performed with LAS X 3.5.2.18963 software (Leica Microsystems, Wetzlar, Germany). For co-localization of *Pantr1* and FOXG1 additional to the Leica system, images were taken with the 60x objective of the BC43 (Oxford Instruments Andor, United Kingdom) and processed with Imaris 10 (Oxford Instruments, United Kingdom).

Bulk RNA-sequencing and RIPseq

Total RNA extracted from mouse hippocampi, cortex or DIV7 primary hippocampal neurons were used for RNAseq. Total RNA extract of FOXG1- and IgG-coIP respectively were used for RIPseq. The cDNA libraries were constructed using TruSeq total RNA sample preparation kit (Illumina, USA), following the manufacturer's

instructions and sequenced on Illumina HiSeq 3000 as paired-end 101 bp reads. For RNAseq, the procedure included depletion of rRNA prior to double-stranded cDNA synthesis and library preparation. Each replicate (n) came from independent cell cultures of different litters respectively from independent mice.

ChIPsequencing

For FOXG1-ChIPseq analysis, wildtype or virally transduced primary hippocampal neurons were fixed and collected as previously described [1], following the instructions of the servicing company (Active Motif, Carlsbad, CA, USA). For FOXG1-ChIPseq analyses after *Pantr1*KD, primary hippocampal neurons transduced with lentiviral shPantr1_1 constructs or control constructs were fixed on DIV7. The FOXG1-ChIPseq of cortical organoids was performed after their fixation using the same protocol as for cells.
A custom Illumina library type on an automated system (Apollo 342, Wafergen Biosystems/Takara) was used to generate ChIPseq libraries, which were subsequently sequenced on Illumina NextSeq 500 or Illumina NovaSeq 6000 (hCO) as single-end 75 bp reads (Active Motif, Carlsbad, CA, USA). Antibodies used for the immunoprecipitation were either anti-FOXG1 (#61211, Active Motif, Carlsbad, CA, USA) for murine samples or anti-FOXG1 (ab18259, abcam, United Kingdom) for human samples.

RNA pulldown of adult hippocampus protein extracts

Pantr1 lincRNA was cloned into pBluescript plasmid such that the sense strand was in frame with T7 promoter and antisense strand with T3. *Pantr1* RNA sense strand was synthesized *in vitro* using linear pBluescript-Pantr1 plasmid (linearized using Xho1 (New England Biolabs, USA)) and T7 RNA polymerase (T7 MEGAscript kit, Thermo Scientific) as per the manufacturer's protocol. Similarly, *Pantr1* antisense strand was synthesized by using Not1 (New England Biolabs, USA) digested linear pBluescript-Pantr1 plasmid and T4 RNA polymerase (T3 MEGAscript kit, Thermo Scientific). Next, 10 µg of *Pantr1* sense RNA were used to label the 3’ end using Pierce™ RNA 3' End Desthiobiotinylation Kit (Thermo Scientific). After labelling, *Pantr1* sense RNA was purified to remove the unincorporated labelled nucleotides and RNA pull down was performed using Pierce™ Magnetic RNA-Protein Pull-Down Kit according to the instructions. Protein extracted from six week old NMRI mouse hippocampus were used for the RNA pull down assay. RNA pulldown samples (n=3) were collected and subjected to LC-MS/MS to identify the proteins interactome of *Pantr1* lincRNA.

Bioinformatics

Single cell RNAsequencing analysis

Reads from single cell (sc)RNAseq were aligned to the GRCh38 human reference genome, and the cell-by-gene count matrices were produced using the RNA STARSolo on the Galaxy Platform. Data were analysed using the Seurat R package v.4.3.0 with R v.4.2.2. The following parameters were used for filtering cells: cut_nUMI <- 500; cut_nGene <- 250; max_nGene <- 8500; cut_log10GenesPerUMI <- 0.80; cut_mito.Ratio <- 0.2; cut_ribo.Ratio <- 0.2.
The expression values were then normalised using the 'SCTransform v2' function. Subsequently, Principal Component Analysis (PCA) was applied to highly variable genes identified by the 'FindVariableGenes' function, retaining the top 40 principal components (PC) based on Seurat's Elbow Plots and determination of percent variation associated with each PC. Clustering was then executed on the PCA-reduced data utilising the 'FindNeighbors' and 'FindClusters' functions, with a resolution set at 0.4. Uniform Manifold Approximation and Projection (UMAP) was employed for dimensionality reduction, providing a visual representation of the data. For cell type annotation, differential expression analysis was conducted between clusters via the 'FindAllMarkers' function, considering genes with a log-fold change greater than 0.1 and an adjusted p-value less than 0.05 as differentially expressed. FOXG1 and *PANTR1* expression levels were plotted using VlnPlot and FeaturePlot functions within the Seurat package. Cell type proportions were calculated using scProportionTest tool with default settings [7].

Bulk RNA-, ChIP-, RIPsequencing analysis

The Galaxy platform as well as R based analysis were used to analyse the RNAseq, FOXG1 ChIPseq and RIPseq data. Mapping was performed on mouse genome build mm10 (GRCm38) or human genome build hg38 depending on organism.
Quality control, trimming, mapping of the RNA sequencing fastq files, and generation of gene-level counts was done on the Galaxy platform [8]. Differential expression analysis of DIV7 hippocampal neurons (Fig. 5B) was done using DESeq2 (1.34.0) on R (4.2.0) on the count matrix output from featurecounts [9]. GO term enrichment analyses were done using clusterProfiler (4.2.2) [10]. Visualisations of volcano plots and heatmaps were done using EnhancedVolcano (1.12.0) and pheatmap (1.0.12) packages, respectively [11-13].
Differential expression analysis for RNAseq of the adult and E18.5 hippocampus sample (Fig. 3C) was done using DESeq2 (v. 1.22.1) [9] on count matrices output from snakePipes (featureCounts, v. 1.6.4) [14]. A linear model controlling for batch effects (e.g., ~batch + treatment or ~ batch + condition) was used and apeglm log2(Fold Change) shrinkage was applied.
RIPseq fastq files were processed on the Galaxy platform. Trimmed and quality filtered reads were aligned to mm10 genome assembly using RNAStar (2.7.10b). FOXG1-coIP reads were normalized to IgG-coIP reads using bamcompare (v. 3.5.4) and the average calculated using bigwigAverage (v. 3.5.4). Differentially immunoprecipitated

RNA was calculated using DESeq2 (v. 2.11.4.0.8) after generating count matrices (featureCounts, v. 2.0.3).
FOXG1 ChIPseq quality controls (FastQC) were performed on the galaxy server (usegalaxy.eu). The sequences were mapped against mm10 with Bowtie and Peaks were called using MACS callpeak. The coverage was calculated followed the analyses as described previously [1].
GO enrichment and differential GO-term analyses were performed using clusterProfiler (v. 4.2.2) [10].
Motif enrichment and differential motif enrichment analyses of the ChIPseq dataset were done using gimmemotifs on Python [15].
Visualisations were done in Galaxy, R (v. 4.1) and Python (v. 3.6). Heatmaps were plotted using heatmap2 (Galaxy Version 3.0.1), venn diagrams using ggVenn (Linlin Yan (2021), ggvenn: Draw Venn Diagram by "ggplot2". R package version 0.1.9) and VennDiagram (Hanbo Chen, VennDiagram: Generate High-Resolution Venn and Euler Plots. R package version 1.7.3. (2022) packages, volcano plots using EnhancedVolcano (BioConductor, v. 3.13) (B. K. Lewis M Rana S., EnhancedVolcano: Publication-ready volcano plots with enhanced colouring and labeling. R package version 1.14.0, (2022)), violin plots using ggplot2 (v. 3.3.5) [16].

Supplemental Table S1*: List of plasmids and their shRNA sequence for lentivirus production*

plasmid carrying the coding sequence with short name (bold)	**sequence for shRNA**	**comment**	**producing company**
pLKO.1-puro-cmv-tGFP sh_Ctrl **shCtrl**	-	used as control for *Foxg1*KD and *Pantr1*KD	MISSION® Luciferase shRNA Control SHC007V MFCD07785395
pLKO.1-puro-cmv-tGFP Sh_Foxg1_1 **shFoxg1_1**	CCG GCC TGA CGC TCA ATG GCA TCT ACT CGA GTA GAT GCC ATT GAG CGT CAG GTT TTT G	for *Foxg1*KD	SIGMA MISSION TRCN0000081746
pLKO.1-puro-cmv-tGFP Sh_Foxg1_2 **shFoxg1_2**	CCG GCT GAC GCT CAA TGG CAT CTA TCT CGA GAT AGA TGC CAT TGA GCG TCA GTT TTT G	for *Foxg1*KD	Cloned by genescript
pLKO.1-puro-cmv tGFP_Sh_Pantr1_1 **shPantr1_1**	CCG GGA ATA ACT GCC ATG GAA GGA TCT CGA GAT CCT TCC ATG GCA GTT ATT CTT TTT TG	for *Pantr1*KD	Sigma MISSION TRCN0000179216

pLKO.1-puro-cmv-tGFP_Sh_Pantr1_2 **shPantr1_2**	CCG GGG GAC AGA GTG CCT AGG TAT CTC GAG ATA CCT AGG CAC TCT GTC CCT TTT TG	for *Pantr1*KD	Cloned by genescript
pLV(Exp)-EGFP:T2A:Puro-U6>LacZ(shRNA_2)-hPGK>mCherry **Ctrl**	-	control for rescue experiment	Cloned and packaged by Vector builder
pLV(Exp)-EGFP:T2A:Puro-U6>FoxG1_shRNA-hPGK>mCherry **shFOXG1_Ctrl**	CCG GCC TGA CGC TCA ATG GCA TCT ACT CGA GTA GAT GCC ATT GAG CGT CAG GTT TTT G	for *Foxg1*KD in rescue experiment	Cloned and packaged by Vector builder
pLV(Exp)-EGFP:T2A:Puro-U6>FoxG1_shRNA-hPGK>(Mouse Pantr1_201) **shFOXG1_Pantr1OE**	CCG GCC TGA CGC TCA ATG GCA TCT ACT CGA GTA GAT GCC ATT GAG CGT CAG GTT TTT G	for *Foxg1*KD and *Pantr1*OE in rescue experiment	Cloned and packaged by Vector builder

Supplemental Table S2: ***List of primers for qRT-PCR***

target	**forward primer**	**reverse primer**
murine Foxg1	AATGACTTCGCAGACCAGCA	CCGGACAGTCCTGTCGTAAA
murine Gapdh	CGGCCGCATCTTCTTGTG	TGACCAGGCGCCCAATAC
murine Pantr1	CGGGACTGTAAGGCGGATAA	GTCCCTCTCCCTCGATGTCA
human ACTIN B	CTGGAACGGTGAAGGTGACA	AAGGGACTTCCTGTAACAATGCA
human PANTR1	CATCAGGGGAGCAACGTGAA	TGTCCTGGGAGGCAGTTAGA
human FOXG1	CTGGCGGCTCTTAGAGAT	CCCTCCCATTTCTGTACGTTT

Supplemental Table S3: ***List of antibodies***

name	**usage and dilution**	**company**
FOXG1	IHC, 1:500	Abcam ab196868
FOXG1	IB, 1:1000, coIP, RIP	active motif #61211
GFAP	IHC, 1:500	life technologies 13-0300
MAP2	ICC, 1:200	Abcam ab32454
NeuN	IHC, 1:150	abcam ab177487
PAX6	IHC, 1:150	BioLegend 901301
TBR1	IHC, 1:200	Abcam ab31940 rabbit

TBR2	IHC, 1:200	Invitrogen 14-4875-82
TUJ-1 (TUBB3)	IHC, 1:200	MMS-435P-100
vGLUT1	IHC, 1:500	Synaptic Systems (SYSYS) 135 303
vGLUT2	IHC, 1:500	Abcam ab79157
anti Mouse-Alexa488	ICC, IHC 1:500	Dianova (715-545-151)
anti Mouse-Alexa594	ICC, IHC 1:500	Dianova (715-585-151)
anti Rabbit-Alexa488	ICC, IHC 1:500	Dianova (711-545-152)
anti Rabbit-Alexa594	ICC, IHC 1:500	Dianova (711-585-152)
anti Rat-Alexa488	ICH, 1:500	ThermoFisher A21208
Streptavidin-Alexa-633	ICC, 1:500	Life Technologies S21375
Tidyblot	IB 1:5000	Biorad Tidyblot

References

1. Akol I, Izzo A, Gather F, Strack S, Heidrich S, D Oh, Villarreal A, Hacker C, Rauleac T, Bella C, Fischer A, Manke T, Vogel T (2023) Multimodal epigenetic changes and altered NEUROD1 chromatin binding in the mouse hippocampus underlie FOXG1 syndrome. Proc Natl Acad Sci U S A 120 (2):e2122467120. doi:10.1073/pnas.2122467120
2. Hebert JM, McConnell SK (2000) Targeting of cre to the Foxg1 (BF-1) locus mediates loxP recombination in the telencephalon and other developing head structures. Dev Biol 222 (2):296-306. doi:10.1006/dbio.2000.9732
3. Vezzali R, Weise SC, Hellbach N, Machado V, Heidrich S, Vogel T (2016) The FOXG1/FOXO/SMAD network balances proliferation and differentiation of cortical progenitors and activates Kcnh3 expression in mature neurons. Oncotarget 7 (25):37436-37455. doi:10.18632/oncotarget.9545
4. Grassi D, Franz H, Vezzali R, Bovio P, Heidrich S, Dehghanian F, Lagunas N, Belzung C, Krieglstein K, Vogel T (2017) Neuronal Activity, TGFbeta-Signaling and Unpredictable Chronic Stress Modulate Transcription of Gadd45 Family Members and DNA Methylation in the Hippocampus. Cereb Cortex 27 (8):4166-4181. doi:10.1093/cercor/bhx095
5. Weise SC, Arumugam G, Villarreal A, Videm P, Heidrich S, Nebel N, Dumit VI, Sananbenesi F, Reimann V, Craske M, Schilling O, Hess WR, Fischer A, Backofen R, Vogel T (2018) FOXG1 Regulates PRKAR2B Transcriptionally and Posttranscriptionally via miR200 in the Adult Hippocampus. Molecular neurobiology:1-14. doi:10.1007/s12035-018-1444-7
6. Chambers SM, Fasano CA, Papapetrou EP, Tomishima M, Sadelain M, Studer L (2009) Highly efficient neural conversion of human ES and iPS cells by dual inhibition of SMAD signaling. Nat Biotechnol 27 (3):275-280. doi:10.1038/nbt.1529

7. Miller SA, Policastro RA, Sriramkumar S, Lai T, Huntington TD, Ladaika CA, Kim D, Hao C, Zentner GE, O'Hagan HM (2021) LSD1 and Aberrant DNA Methylation Mediate Persistence of Enteroendocrine Progenitors That Support BRAF-Mutant Colorectal Cancer. Cancer Res 81 (14):3791-3805. doi:10.1158/0008-5472.CAN-20-3562
8. Afgan E, Baker D, Beek M, Blankenberg D, Bouvier D, Cech M, Chilton J, Clements D, Coraor N, Eberhard C, Grüning B, Guerler A, Hillman-Jackson J, Von Kuster G, Rasche E, Soranzo N, Turaga N, Taylor J, Nekrutenko A, Goecks J (2016) The Galaxy platform for accessible, reproducible and collaborative biomedical analyses: 2016 update. Nucleic Acids Research 44 (W1):W3. doi:10.1093/nar/gkw343
9. Love MI, Huber W, Anders S (2014) Moderated estimation of fold change and dispersion for RNA-seq data with DESeq2. Genome Biol 15 (12):550. doi:10.1186/s13059-014-0550-8
10. Wu T, Hu E, Xu S, Chen M, Guo P, Dai Z, Feng T, Zhou L, Tang W, Zhan L, Fu X, Liu S, Bo X, Yu G (2021) clusterProfiler 4.0: A universal enrichment tool for interpreting omics data. Innovation (Camb) 2 (3):100141. doi:10.1016/j.xinn.2021.100141
11. Kolde R (2019) pheatmap: Pretty Heatmaps. 1.0.12 edn.,
12. Blighe K, Rana S, Lewis M (2018) EnhancedVolcano: Publication-ready volcano plots with enhanced colouring and labeling.
13. Galaxy C (2022) The Galaxy platform for accessible, reproducible and collaborative biomedical analyses: 2022 update. Nucleic Acids Res 50 (W1):W345-W351. doi:10.1093/nar/gkac247
14. Liao Y, Smyth GK, Shi W (2014) featureCounts: an efficient general purpose program for assigning sequence reads to genomic features. Bioinformatics 30 (7):923-930. doi:10.1093/bioinformatics/btt656
15. van Heeringen SJ, Veenstra GJ (2011) GimmeMotifs: a de novo motif prediction pipeline for ChIP-sequencing experiments. Bioinformatics 27 (2):270-271. doi:10.1093/bioinformatics/btq636
16. Wickham H (2016) ggplot2: Elegant Graphics for Data Analysis. Use R! Springer Cham. doi:10.1007/978-3-319-24277-4